JOURNAL OF AGRICULTURAL AND FOOD CHEMISTRY



# Interactions between a Non Glycosylated Human Proline-Rich Protein and Flavan-3-ols Are Affected by Protein Concentration and Polyphenol/Protein Ratio

CHRISTINE PASCAL,[†] CÉLINE PONCET-LEGRAND,[†] ANNE IMBERTY,[‡] CATHERINE GAUTIER,[‡] PASCALE SARNI-MANCHADO,[†] VÉRONIQUE CHEYNIER,[†] AND AUDE VERNHET*,[†]

UMR INRA−Montpellier SupAgro 1083 Sciences Pour l'Oenologie, 2 place Pierre Viala, F-34060 Montpellier, France, and Centre de Recherches sur les Macromolécules Végétales, Centre National de la Recherche Scientifique (affiliated with Université Joseph Fourier and belonging to ICMG), B.P. 53, F-38041 Grenoble cedex 9, France

Interactions between salivary proline-rich proteins and tannins are involved in astringency, which is one of the most important organoleptic sensations perceived when drinking wine or tea. This work aimed to study interactions between a recombinant human salivary proline-rich protein, IB-5, and a flavan-3-ol monomer, epigallocatechin gallate (EGCG). IB-5 presented the characteristics of natively unfolded proteins. Interactions were studied by dynamic light scattering, isothermal titration microcalorimetry, and circular dichroism. The interaction mechanism was dependent on protein concentration. At low concentrations, a three-stage mechanism was evidenced. Saturation of the interaction sites (first stage) was followed by protein aggregation into metastable colloids at higher EGCG/protein ratios (second stage). Further increasing this ratio led to haze formation (third stage). At low ratios, a disorder-to-order transition of IB-5 structure upon binding was evidenced. At high protein concentrations, direct bridging between proteins and EGCG was observed, resulting in significantly lower aggregation and turbidity thresholds.

**KEYWORDS: PRPs; proline-rich proteins; IB-5; natively unfolded proteins; PPII helices; flavan-3-ols; EGCG; isothermal titration microcalorimetry; dynamic light scattering; circular dichroism; disorder-to-order transition.**

## INTRODUCTION

Polyphenols such as tannins are widespread in the plant kingdom and they are known in particular to participate in plant defense mechanisms (*1*−*3*). Tannins have antioxidant properties, which may be beneficial against illnesses that are due to oxidative stress (*4*). They also have negative effects on animals, including growth rate depression and inhibition of digestive enzymes (*3*, *5*, *6*). These biological effects are related to the ability of tannins to interact with proteins and sometimes to precipitate them (*7*). Our interest is focused on tannin interactions with salivary proline-rich proteins, which are thought to be part of animal and human defense mechanism against dietary tannins (*6*, *8*−*10*). Interactions between salivary proline-rich proteins and tannins also seem to be responsible for astringency perception (*3*, *11*−*14*), which is one of the major organoleptic characteristics of plant-made beverages (wine, tea, beer, fruit juice, etc.). We focused here on red wine astringency that can be considered as a quality or a default, depending on the wine type. Astringency is often modulated by an enological process called "fining". Several types of fining agents such as casein, albumin, or gelatin can be added to the wine in order to make some tannins precipitate. This enological operation is often achieved empirically and the result is evaluated by tasting the wine. A better understanding of molecular and colloidal causes of these interactions could facilitate astringency control, which is of importance in the wine industry.

Tannins present a wide range of structures usually divided into two categories: hydrolyzable and condensed tannins. The hydrolyzable tannins are compounds containing a central core of glucose or other polyhydric alcohol acylated with gallic acid (gallotannins) or hexahydroxydiphenic acid (ellagitannins). The condensed ones are oligomers and polymers of flavan-3-ols that may differ in the nature and proportions of their constitutive units (e.g., catechin, epicatechin, epicatechin gallate, epigallocatechin), in their degree of polymerization (varying between 2 and more than 100), and in the type of linkages between units. Tannins in wines are flavan-3-ols.

Proline-rich proteins (PRPs) constitute about two-thirds of human parotid salivary proteins (*15*, *16*). They are usually

* Corresponding author: tel + 33 499 612 758; fax + 33 499 612 857; e-mail vernhet@supagro.inra.fr.
[†] INRA−Montpellier SupAgro.
[‡] CERMAV-CNRS.

10.1021/jf0704108 CCC: $37.00 
Published on Web 05/16/2007

divided into glycosylated, acidic, and basic types, which have different functions (*17*). Acidic PRPs are reported to bind calcium and to inhibit crystal growth, functions that may be important in maintaining calcium homeostasis in the mouth (*7*). They are also involved in dental pellicle (*7*). Glycosylated PRPs ensure oral lubrication (*18*) and bind oral bacteria (*19*). Basic PRPs are able to interact with plant tannins, as stated before. Among basic PRPs, IB-5 is encoded by the *PRB4S* gene: it is the C-terminal part of the PRB4S proprotein, which is cleaved in the salivary glands by furin-like proteases to generate IB-5 and a glycosylated protein II-1 (*17*). IB-5 contains 70 amino acids arranged in six tandem repeats (**Figure 1**). We produced this protein by the recombinant pathway using the yeast *Pichia pastoris*, as previously described (*20*). This protein was shown to be a natively unfolded protein (*20*), that is, a protein presenting very little secondary structure and, as a consequence, a flexible backbone (*21*, *22*).

Interactions between tannins and proline-rich proteins have been investigated with numerous complementary techniques such as nuclear magnetic resonance (NMR) (*10*, *23*−*25*), small-angle X-ray scattering (SAXS) (*26*), dynamic light scattering (DLS) (*26*, *27*), mass spectrometry (MS) (*25*, *28*), and, more recently, isothermal titration microcalorimetry (ITC) (*29*, *30*). These interactions primarily generate noncovalent complexes. They increase with both the degree of polymerization of the tannins and their extend of galloylation. Interactions are generally attributed to hydrophobic interactions between the aromatic rings of the tannins and hydrophobic sites of the protein, such as prolyl rings of proline residues. Hydrogen bonding between the H-acceptor sites of the proteins and the hydroxyl groups carried by polyphenols is also reported to strengthen these interactions.

Using proline-rich peptides of 7 and 19 amino acids, histatins and polyphenols (flavan-3-ol monomers and hydrolyzable tannins), Charlton et al. (*31*) proposed a three-step mechanism of interaction as a function of the flavan-3-ol/protein ratio. At low ratios, "soluble complexes" are formed after binding of polyphenols to proteins. When the flavan-3-ol/protein ratio increases, proteins are cross-linked by polyphenols and the complexes become insoluble (second stage). Finally, the third stage corresponds to further aggregation of proteins and leads to phase separation. Jobstl et al. (*26*) confirmed this mechanism using a $\beta$-casein that was dephosphorylated, so as to present a random coil structure, and epigallocatechin gallate (EGCG). In the present work, we studied the interactions between the full-length non glycosylated human salivary proline-rich protein IB-5 and a flavan-3-ol monomer, EGCG. Our aim was to determine the interaction mechanism between IB-5 and EGCG with the use of three complementary methods: DLS, ITC, and CD. Over the impact of EGCG/IB-5 molar ratio, we evaluated the influence of protein concentration and we took into account kinetic effects.

## MATERIALS AND METHODS

**Chemicals.** EGCG was purchased from Sigma−Aldrich (St. Louis, MO); sodium hydroxide, hydrochloric acid, and sodium chloride were purchased from Merck (Whitehouse Station, NJ). Human salivary proline-rich protein, IB-5, was produced by use of the yeast *P. pastoris* as a host organism and purified as described previously (*20*). N-terminal sequencing of the protein evidenced the presence of two sequences in the protein sample, respectively corresponding to IB-5 N-terminal sequence and to the same sequence with three more amino acids (*20*). MALDI TOF mass spectrometry corroborated the presence in the sample of a protein with a molecular mass of 6923 Da (IB-5) and another one of 7237 Da (IB-5 with three more amino acids S, A, and R on its N-terminal end). This protein mixture was considered as relevant for studying PRP/flavan-3-ol interactions, as there is no major interaction site in the three additional amino acids. It will be referred here as "IB-5". To get indicative molar concentrations of the protein solutions, a mean molecular mass of 7000 Da for the protein was used in the calculations. Nevertheless, protein concentration will always be indicated in milligrams per milliliter in this paper.

```
1    SPPGKPQGPPQQE
14     GNKPQGPPPP
24      GKPQGPPPA
33     GGNPQQPQAPPA
45     G KPQGPPPPPQ
56     GGRPPRPAQGQQPPQ
```

**Figure 1.** IB-5 amino acid sequence (*20*), displaying the tandem repeats.

**Sample Preparation.** The whole experiments were performed at an acidic pH of 3.5, which is the average pH of wine. We previously checked that, when drinking wine, the pH of the expectorated solution is equal to that of wine and not to that of saliva (neutral pH). Ionic strength was first adjusted to 100 mM with NaCl, which is consistent with wine (*32*) and saliva (*33*) mean ionic strengths.

Stock solutions of protein (2 and 5 mg·mL$^{-1}$) and of EGCG (4.0, 8.0, and 12.8 mM) were prepared in the interaction medium (aqueous solution at pH 3.5 adjusted with HCl, plus 100 mM NaCl). They were immediately frozen (−20 °C) to prevent EGCG oxidation and protein proteolysis. Prior to mixing, they were diluted at room temperature to the requested concentration and filtered with disposable syringe filters [Millipore, poly(vinylidene difluoride) (PVDF) membrane, 0.22 $\mu$m].

**Dynamic Light Scattering:** *Protein Dissolution.* DLS is a light-scattering experiment in which the statistical intensity fluctuations in light scattered from colloids in solution are measured. These fluctuations are related to their Brownian motion (and so to their diffusion coefficient). Their analysis provides information concerning particle size and polydispersity. DLS measurements on protein solutions were carried out with a Zetasizer Nano S (Malvern Instruments, Malvern, U.K.), equipped with a 4 mW He−Ne laser (633 nm). Measurements were performed at 25 °C, at an angle of 173° from the incident beam. The time dependence of the scattered light was monitored and the autocorrelation function was recorded. Cumulant analysis was achieved to fit the autocorrelation curves and to calculate the diffusion coefficient ($D$) of the colloids. Hydrodynamic radii $R_h$ were then derived from the diffusion coefficient by use of the Stokes−Einstein equation, with the assumption that objects are spherical: $D = kT/(6\pi\eta R_h)$, where $k$ is the Boltzmann constant, $T$ is the temperature, and $\eta$ is the solvent viscosity. Peak analysis in volume was considered and the corresponding hydrodynamic diameters were referred to as $Z_{av}$. Measurements were performed in duplicate on several protein concentrations (from 3 to 5 mg·mL$^{-1}$) to extrapolate $Z_{av}$ to null concentration.

*Protein/EGCG Interaction Kinetics.* Protein/EGCG interactions were monitored with a Malvern Autosizer 4800 (Malvern Instruments, Malvern, U.K.) equipped with a 35 mW He−Ne laser (633 nm, Coherent, Auburn, CA) and APD detection. Measurements were carried out at 25 °C, at an angle of 90° from the incident beam. Peak intensity analyses were used to determine the average hydrodynamic diameters of the aggregates, $Z_{av}$. Polydispersity index was obtained by a cumulant analysis of the intensity autocorrelation function. Time zero was defined as solution mixture in the measurement cell, and mixture evolution was monitored for 24 h. Each measurement was the average of 10 subruns, and all assays were performed in duplicate. Control measurements were made on solvent, and on proteins or EGCG solutions at adequate concentrations.

**Isothermal Titration Microcalorimetry**. In a typical ITC experiment, a solution of a ligand (receptor, antibody, etc.) is titrated against a solution of a binding partner at constant temperature. The heat released or absorbed upon their interaction ($\Delta H$) is monitored over time. Raw data are obtained as a plot of heat flow (microcalories per second) against time (minutes). These raw data are then integrated peak-by-peak and normalized to obtain a plot of observed enthalpy change per mole of injectant ($\Delta H$, kilocalories per mole) against the molar ratio ligand/binding partner. Experiments were conducted on a VP ITC microcalorimeter (Microcal, Northampton, MA) at 25 °C. EGCG

solution (6.4 or 12.8 mM) was titrated into the stirred sample cell (1448 $\mu$L) containing the protein (0.25−2 mg·mL$^{-1}$) as a sequence of 30 injections of 10 $\mu$L. Reverse titration was also achieved when necessary. The duration of each injection was 20 s, and a delay time of 300 s was respected between injections to allow equilibration. Data acquisition was achieved with VP Viewer 2000 software. Dilution of EGCG signal was recorded and subtracted from interaction raw data. By use of the Origin 7 software, raw data were integrated peak by peak and normalized to get a plot of observed enthalpy change per mole of injectant ($\Delta H_{obs}$) against EGCG/protein molar ratio.

**Circular Dichroism.** Far ultraviolet (200−260 nm) circular dichroism spectra were recorded on a Chirascan circular dichroism spectrometer (Applied Photophysics, Leatherhead, U.K.) at room temperature in a circular cell (0.5 mm length path). All spectra were averaged from five scans. The EGCG spectrum was recorded as a control and subtracted from the EGCG/protein mixture spectrum. The protein concentration was fixed at 0.5 mg·mL$^{-1}$, and the EGCG/IB-5 molar ratio at 6.

## RESULTS AND DISCUSSION

Protein concentration in the following experiments ranged from 0.2 to 2 mg·mL$^{-1}$. Indeed, PRP concentration in saliva is reported to be around 1.5 mg·mL$^{-1}$ (*34*), and we estimated the dilution of saliva in the mouth when drinking wine to be around 6-fold. Such a dilution leads to a final PRP concentration on the order of 0.2 mg·mL$^{-1}$ in the wine/saliva mixture.

**DLS Experiments**. Protein dissolution in 100 mM NaCl was checked for a concentration range between 3 and 5 mg·mL$^{-1}$. DLS experiments evidenced the presence of very few particles in these rather concentrated protein solutions (diameter around 100 nm), attributed to the presence of some residual aggregates. These particles, which represented less than 1% of the scattered intensity in volume, accounted for only a negligible amount of the protein content. They could be eliminated neither by filtration on 0.22 $\mu$m filters nor by ultracentrifugation (100000*g*, 15 h). Average hydrodynamic diameter of IB-5, extracted from the size analysis in volume, was 3.4 ± 0.2 nm. Within the tested concentration range, it did not depend on protein concentration. Distribution around this average value was quite large (result not shown). This can be explained by the probable asymmetry of unfolded proteins and their random orientations in the sample. In such cases, hydrodynamic diameter is considered only as a convenient or conventional magnitude to characterize the size distribution in solutions (*35*).

Protein/EGCG interactions were studied by DLS for three protein concentrations (0.2, 0.5, and 1 mg·mL$^{-1}$) and several EGCG/protein molar ratios (3−60). Controls were recorded on IB-5 and EGCG solutions at the different concentrations used. The intensity scattered by these solutions remained very low (normalized scattering intensity $I_{scatt} < 1$). We therefore concluded that when an increase in scattered intensity was observed after EGCG addition to IB-5, aggregates made of several EGCG and IB-5 molecules were formed. These aggregates may be compared to what Charlton et al. (*31*) called "insoluble complexes". Aggregate formation and evolution were monitored during 24 h except when the medium became turbid. Turbidity results from the presence in solution of numerous aggregates or of large ones. The different behaviors observed during interaction experiments are summarized in **Figure 2**. They indicate that interaction mechanisms were dependent on both protein concentration and EGCG/IB5 molar ratio.

At low protein concentration (0.2 mg·mL$^{-1}$), three different behaviors were observed (**Figure 2**). At low molar ratios, no significant variation in scattered intensity could be observed. If interactions between IB-5 and EGCG occurred, they did not lead to the formation of detectable aggregates. The aggregation

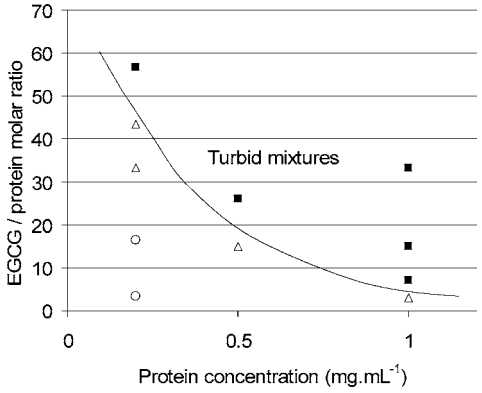


**Figure 2.** Phase diagram corresponding to EGCG/IB-5 mixtures in HCl, pH 3.5, and 100 mM NaCl. (○) Mixtures in which no colloids detected by DLS; (△) mixtures containing stable colloids; (■) turbid mixtures.

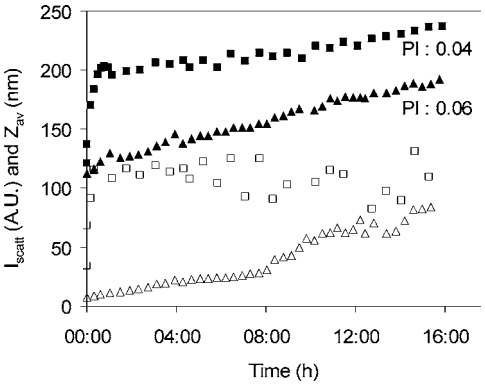


**Figure 3.** DLS monitoring of IB5/EGCG mixtures for (triangles) 0.2 mg·mL$^{-1}$ IB-5 and 1 mM EGCG (EGCG/protein molar ratio = 36) and (squares) 0.2 mg·mL$^{-1}$ IB-5 and 1.3 mM EGCG (EGCG/protein molar ratio = 46). Open symbols correspond to normalized scattered intensities ($I_{scatt}$, absorbance units), and solid ones correspond to mean hydrodynamic diameters ($Z_{av}$, nanometers).

threshold was found to be between EGCG/protein molar ratios of 18 and 36. At a ratio of 36, aggregation was evidenced immediately after mixing (**Figure 3**). The hydrodynamic diameter of the aggregates, $Z_{av}$, increased slowly, in parallel to the scattered intensity. At a ratio of 46, both aggregate size and scattered intensity quickly reached pseudoplateau values, indicating that aggregation occurred faster (**Figure 3**). In both cases, polydispersity indexes (PI) remained low. Suspensions were metastable and no phase separation (haze formation) could be observed. Further increasing the EGCG concentration led to immediate haze formation, corresponding to enlarged aggregation in solution. The threshold to reach this stage was called the "turbidity threshold". At a protein concentration of 0.2 mg·mL$^{-1}$, the turbidity threshold was found to be between 46 and 57 EGCG/protein. These results are in accordance with the three-stage mechanisms proposed by Charlton et al. (*31*) and Jobstl et al. (*26*).

Increasing IB-5 concentration significantly decreased both aggregation and turbidity thresholds (**Figure 2**). At high protein concentration (1 mg·mL$^{-1}$), aggregation occurred for a molar ratio of 3 EGCG/protein. At this ratio, metastable aggregates were observed ($Z_{av}$ on the order of 180 nm, $I_{scatt}$ 40, PI 0.17). This may be due to a direct bridging of proteins by EGCG, favored by the increasing protein concentration (when proteins are more concentrated, they are nearer in the solution).

**ITC Experiments.** DLS experiments were unable to prove that an interaction took place at low EGCG/protein molar ratios

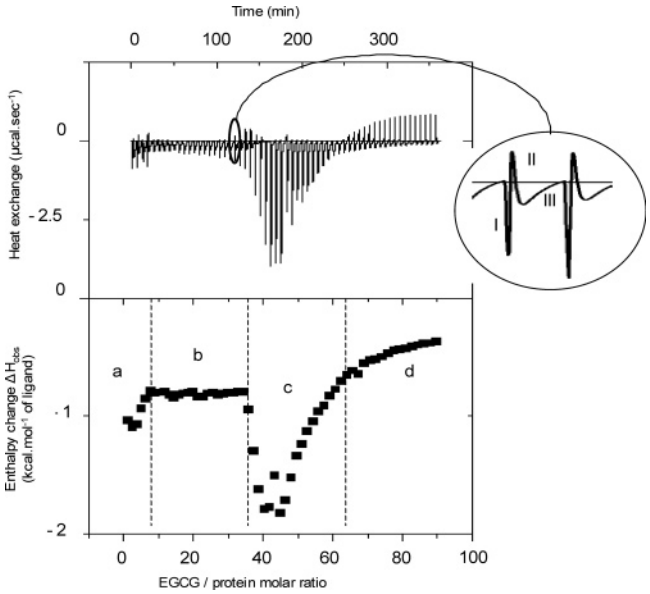


**Figure 4.** ITC raw data and enthalpy change per mole of injectant ($\Delta H_{obs}$) against EGCG/protein molar ratio for titration of 0.5 mg·mL$^{-1}$ IB-5 by 12.8 mM EGCG. Letters a–d correspond to different stages of the titration. (Inset) I, first exothermic signal; II, endothermic signal; III, second exothermic signal.

**Table 1.** EGCG/Protein Molar Ratio Threshold for Third Interaction as a Function of IB-5 Concentration

| protein concentration (mg·mL$^{-1}$) | 0.25 | 0.375 | 0.5 |
|---|---|---|---|
| (EGCG/protein) ratio 3rd stage threshold | >70 | 40 | 33 |

and at low protein concentration, as no aggregation was detected. Therefore, we checked the existence of a binding phenomenon by ITC. Moreover, this technique can provide thermodynamic data for this system.

Experiments were achieved at five IB-5 concentrations (0.25, 0.375, 0.5, 1, and 2 mg·mL$^{-1}$). Their results corroborated the effect of protein concentration on the mechanism of interaction. ITC raw data at high protein concentrations (1 and 2 mg·mL$^{-1}$) were not interpretable. This is likely to be due to the immediate aggregation of EGCG and IB-5, as observed by DLS.

At the three lowest concentrations, the raw data presented the same enthalpy change profile. Results are reported in **Figure 4** for a protein concentration of 0.5 mg·mL$^{-1}$. Unfortunately, we could not derive thermodynamic data from our system because of the complexity of the signal. Four phases (**Figure 4a**−**d**) were observed during the titration. At the beginning of the titration and until the EGCG/protein molar ratio reached a value around 10 (**Figure 4a**), $\Delta H_{obs}$ increased. The binding isotherm presented a sigmoid shape as if site saturation had been reached. This signal shows that an interaction between EGCG and IB-5 took place. In the second phase (**Figure 4b**), $\Delta H_{obs}$ was stable and slightly negative, therefore indicating a weak exothermic phenomenon. In the third phase (**Figure 4c**), a complex shape was observed for the isotherm, with exothermic peaks of increasing and then decreasing amplitude. The threshold to reach this third stage was dependent on protein concentration (**Table 1**). This implies that the observed phenomenon does not deal with protein saturation. Moreover when this stage was observed (titration of IB-5 at 0.375 and 0.5 mg·mL$^{-1}$), the titration mix was always turbid at the end of titration, indicating extensive aggregation. This third phase was not observed for an IB-5 concentration of 0.25 mg·mL$^{-1}$ because of the low

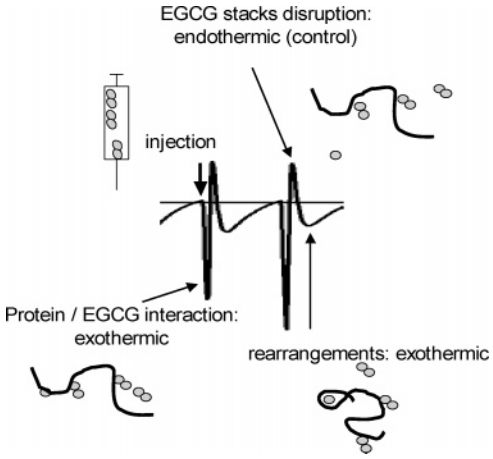


**Figure 5.** Interpretation of the complex signal observed in ITC at each injection in the first two phases of the titration. Bold arrow indicates the moment of injection on the ITC raw data. Circles represent EGCG molecules (isolated or stacked); bold line represents the unstructured protein. Phenomena occur quite simultaneously in the medium but when one supplants the others, its intensity is determinant for the overall signal that is recorded as raw data.

concentration of added EGCG. At the end of the titration, we observed an endothermic phenomenon (**Figure 4d**), which was attributed to EGCG dilution. Indeed, EGCG is likely to self-associate in aqueous solution (*36*, *37*). As EGCG is very concentrated in the syringe before injection, molecules are probably stacked. A control experiment was performed (Supporting Information). It confirmed that injection of EGCG in the titration medium yielded endothermic peaks that were probably caused by the dissociation of EGCG stacks.

During the first two stages described above (**Figure 4a**,**b**), the signal observed at each EGCG injection (**Figure 4**, inset) was complex and corresponded to successive heat absorption and release. This signal results from different concomitant phenomena, the respective intensity of the most important one being determinant for the resultant intensity that is recorded as raw data. Heat absorption (**Figure 4**, inset, peak II) was related to EGCG dilution into the solvent, as stated before. Heat release was attributed to EGCG/protein interactions. The first release (**Figure 4**, inset, peak I) corresponds to the first interactions, and the second one (**Figure 4**, inset, peak III), which is less important and less sharp, corresponds to inter- and intramolecular rearrangements after EGCG dilution. Indeed, after partial disruption of EGCG stacks, more EGCG molecules may be able to interact with proteins in the medium (**Figure 5**). To check this hypothesis, reverse titration was achieved: EGCG was placed in the measurement cell and titrated by IB-5. In this case, as the volume increase at each injection is low (less than 0.7%), EGCG dilution is negligible and engenders little enthalpy change. Successive heat absorption and release were not observed (Supporting Information), confirming that these rearrangements are a consequence of EGCG stack disruption.

ITC data corroborated the existence of a three-stage mechanism at low protein concentration. The first interaction phase, which has a sigmoidal shape on the enthalpy change profile, seems to correspond to the saturation of the protein interaction sites taking place at EGCG/protein molar ratios above 10. Even if several authors showed that other residues may be involved in the binding process between PRPs and polyphenols (*10*, *25*, *31*), proline residues are usually considered as the main interaction sites (*12*, *14*, *23*, *24*). Among the 29 prolines of IB-5, seven residues are isolated while the other ones are present

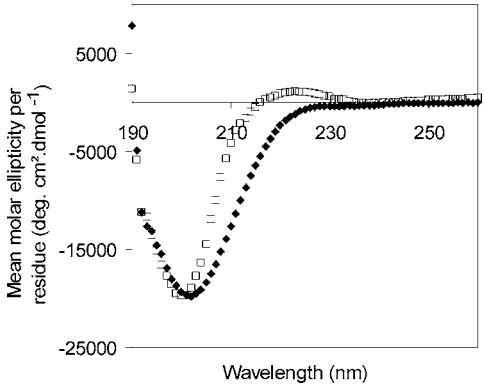


**Figure 6.** Circular dichroic spectra of (◆) IB-5 and (□) mixture of IB-5 and EGCG after subtraction of EGCG signal (EGCG/protein molar ratio = 6) recorded in 100 mM NaCl.

in eight "proline sequences" corresponding to a succession of several (2−5) proline residues (**Figure 1**). Because of steric hindrance, all the residues in the proline sequences may not be able to interact with EGCG in the present case and the isolated prolines situated near proline sequences may not either. Therefore, saturation of the binding sites at 10 EGCG/protein seems to be reasonable. NMR investigations are needed to determine which amino acids are involved in PRP−EGCG interactions and to get the exact saturation threshold. No aggregation occurred during this first phase, as shown by DLS (EGCG/protein <10). The second phase begins after saturation of the protein sites and is likely to correspond to bridging of proteins by EGCG molecules. Even if the interactions sites are saturated, EGCG molecules can also interact together (hydrophobic stacks) and provoke protein aggregation. This phenomenon leads to the formation of the metastable aggregates that were observed by DLS. The bell-shaped curve observed in the last stage can be attributed to an enlarged aggregation, leading to turbidity.

**CD Experiments**. Additional experiments at low IB-5 concentration and low EGCG/protein ratio were conducted to check the effect of EGCG binding on the protein secondary structure. IB-5 presents the characteristics of a natively unfolded protein. It already has been assessed that unfolded peptides have significant amounts of poly(L-proline) II helices (PPII) in the form of short helical regions (*38*, *39*) and that such preformed structural elements could be of importance in partner recognition when binding (*40*). Moreover, this kind of proteins may undergo a folding process upon binding (*39*, *41*, *42*).

The IB-5 circular dichroic spectrum (**Figure 6**) was consistent with natively unfolded protein nature (*39*), as expected for salivary proline-rich proteins (*21*). This spectrum presented a deep minimum near 200 nm and molar ellipticity close to zero in the vicinity of 222 nm. It resembles the spectrum of PPII helices that has a more pronounced minimum (approximately −20 000 deg·cm²·dmol⁻¹) than random coil ones (−5000 deg·cm²·dmol⁻¹) (*39*). Nevertheless, it did not present a positive band in the region of 220−230 nm, as expected for PPII, and this absence reflected a higher extent of disorder compared to that of PPII structure.

EGCG asymmetric carbon interacts with circularly polarized light, resulting in a non-null CD spectrum (*43*). This spectrum was used as a control and subtracted from that of the EGCG/protein mixture. IB-5 CD spectrum was modified after addition of EGCG at an EGCG/protein molar ratio of 6 (ratio corresponding to the first interaction stage determined by DLS and ITC). A positive band appeared in the 215−230 nm region

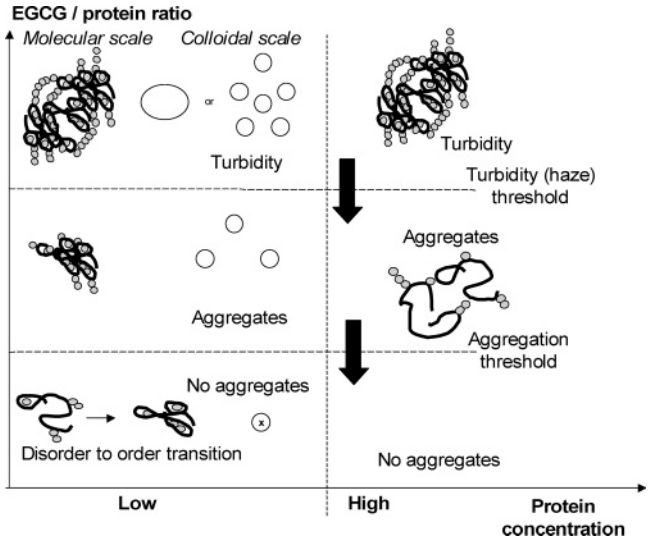


**Figure 7.** Proposed mechanisms of interaction between IB-5 and EGCG. Gray circles represent EGCG molecules and bold lines represent IB-5 proteins. (○) Colloidal aggregates.

replacing the negative shoulder. This corresponds to a higher extent of structure (disorder to order transition) (*39*) and indicates that IB-5 secondary structure was modified upon EGCG binding.

This disorder-to-order transition has not been reported before. Simon et al. (*25*) and Jobstl et al. (*26*), who also studied interactions between PRPs and tannins using CD measurements, did not observe any structural modification of the proteins. However, this is not in contradiction with present results. Simon et al. (*25*) used a flavan-3-ol dimer ($B_3$) and a salivary proline-rich peptide (IB-$7_{14}$). This peptide (14 amino acids) may have been too short to observe a conformational modification by a global method such as CD. Nevertheless, molecular modeling showed a conformational dynamic restriction of the peptide. Since IB-$7_{14}$ sequence is present three times in IB-5 with more than 80% identity, the molecular modeling results are of interest to understand IB-5 behavior and this dynamic restriction may be the initial process of the disorder-to-order transition that was shown here. Jobstl et al. (*26*) used dephosphorylated bovine $\beta$-casein, which is a 209 amino acid long protein that adopts an extended conformation after dephosphorylation. However, this protein contains less proline residues (16%) than IB-7 or IB-5 (40%) and does not present tandem repeats in its sequence, which can be of importance for the interaction mechanism and strength (*23*, *44*). These tandem repeats may also be required to observe the conformational transition.

**Proposed Interaction Mechanism between IB-5 and EGCG.** The experiments that were conducted here allowed us to propose a mechanism of interaction between EGCG and a full-length salivary PRP (**Figure 7**). In conditions of low protein concentrations, this mechanism is consistent with those proposed by other authors for the interactions between denatured proteins/peptides and flavan-3-ols (*26*, *31*). At low EGCG/protein ratios, EGCG progressively coats the protein but no aggregation occurs. At higher ratios, EGCG bridges the coated proteins, which provokes the appearance of aggregates in the medium. Still increasing the molar ratio, the formation of numerous colloids or of large ones renders the solution turbid (haze formation). Additionally, a protein disorder-to-order transition was observed during the first interaction phase. We also underlined an effect of IB-5 concentration on this mechanism. At high protein concentration, EGCG bridges proteins well before saturation of the interaction

sites, leading to aggregation from much lower EGCG/protein ratios. The turbidity threshold is thus also significantly decreased. Previous works already evidenced that less tannin was required to precipitate proteins from concentrated solutions than from dilute ones (*29*, *45*). This was attributed to intermolecular cross-linking between interaction sites of adjacent proteins by tannins, favored in concentrated protein solutions. Such an influence of the protein concentration was also evidenced by Poncet-Legrand et al. (*27*) on poly(L-proline)/flavan-3-ol monomer model systems.

The effect of protein concentration on the mechanism of interaction seems to point out the extreme adaptability of salivary proline-rich proteins to improve human protection against dietary tannins. Indeed, they may allow proteins to scavenge most of the tannins in the mouth, preventing inhibition of enzymes in the digestive track.

## ABBREVIATIONS USED

CD, circular dichroism; DLS, dynamic light scattering; EGCG, epigallocatechin gallate; ESI MS, electrospray ionization mass spectrometry; ITC, isothermal titration microcalorimetry; NMR, nuclear magnetic resonance; MALDI TOF, matrix-assisted laser desorption ionization/time of flight; PPII, poly(L-proline) II; PRPs, proline-rich proteins; SAXS, small-angle X-ray scattering.

## ACKNOWLEDGMENT

We thank Nathalie Declerck and Yannick Bessin (CBS Montpellier) for their help with CD spectroscopy and Marie José Vallier and Thérèse Marlin (INRA Montpellier) for their technical support in protein purification.

**Supporting Information Available:** Two figures corresponding to (a) ITC raw data for titration of 12.8 mM EGCG by 1 $mg \cdot mL^{-1}$ IB-5 and (b) ITC raw data for EGCG dilution. This material is available free of charge via the Internet at http://pubs.acs.org.

## LITERATURE CITED

(1) Hagerman, A. E.; Robbins, C. T. Implications of soluble tannin−protein complexes for tannin analysis and plant defense mechanisms. *J. Chem. Ecol.* **1987**, *13*, 1243−1259.

(2) Clausen, T. P.; Reichardt, P. B.; Bryant, J. P.; Provenza, F. Condensed tannins in plant defense: A perspective on classical theories. In *Plant polyphenols*; Hemingway, R. W., Lacks, P. E., Eds.; Plenum Press: New York and London, 1992; pp 639−651.

(3) Bennick, A. Interaction of plant polyphenol with salivary proteins. *Crit. Rev. Oral Biol. Med.* **2002**, *13*, 184−196.

(4) Manach, C.; Scalbert, A.; Remesy, C.; Morand, C. Consommation et biodisponibilité des polyphénols. In *Sciences et Techniques Agroalimentaires*, Technique et Documentation ed.; Sarni-Manchado, P., Cheynier, V., Eds.; Lavoisier: Londres, Paris, and New York, 2006; pp 361−390.

(5) Butler, L. G. Antinutritional effects of condensed and hydrolyzable tannins. In *Plant Polyphenols*; Hemingway, R. W., Lacks, P. E., Eds.; Plenum Press: New York, 1992; pp 693−698.

(6) Mehansho, H.; Butler, L. G.; Carlson, D. M. Dietary tannins and salivary proline-rich proteins: Interactions, induction, and defense mechanisms. *Annu. Rev. Nutr.* **1987**, *7*, 423−440.

(7) Bennick, A. Salivary proline-rich proteins. *Mol. Cell. Biochem.* **1982**, *45*, 83−99.

(8) Butler, L. G.; Mole, S. Salivary proline-rich tannin-binding proteins as a defense against dietary tannins. *Bul. Liaison−Groupe Polyphénols* **1988**, 111−1174 (Compte Rendu JIEP88, St. Catharine, Ontario, Canada).

(9) Charlton, A. J.; Baxter, N. J.; Haslam, E.; Williamson, M. Salivary proteins as a defense against dietary tannins. In *Polyphenols in food*; Amado, R., Andersson, H., Bardocz, S., Serra, F., Eds.; Office for Official Publications of the European Communities: Luxembourg, 1998; pp 179−185.

(10) Baxter, N. J.; Lilley, T. H.; Haslam, E.; Williamson, M. P. Multiple interactions between polyphenols and a salivary proline-rich protein repeat results in complexation and precipitation. *Biochemistry* **1997**, *36*, 5566−5577.

(11) Beeley, J. A. Basic proline-rich proteins: multifunctional defence molecules? *Oral Dis.* **2001**, *7*, 69−70.

(12) Cheynier, V.; Sarni-Manchado, P. Structures phénoliques et goût. In *Les polyphénols en agroalimentaire*, Technique et Documentation ed.; Sarni-Manchado, P., Cheynier, V., Eds.; Lavoisier: Londres, Paris, and New York, 2006; pp 89−134.

(13) Gawel, R. Red wine astringency : a review. *Aust. J. Grape Wine Res.* **1998**, *4*, 74−95.

(14) Haslam, E.; Williamson, M. P.; Baxter, N. J.; Charlton, A. J. Astringency and polyphenol protein interactions. In *Phytochemicals in human health protection*; Romeo, J. T., Ed.; Kluwer Academic/Plenum Publishers: New York, 1999; pp 289−318.

(15) Azen, E. A.; Amberger, E.; Fisher, S.; Prakobphol, A.; Niece, R. L. PRB1, PRB2, and PRB4 coded polymorphisms among human salivary concanavalin-A binding, II-1, and Po proline-rich proteins. *Am. J. Hum. Genet.* **1996**, *58*, 143−153.

(16) Edgar, W. M. Saliva: its secretion, composition and functions. *Br. Dent. J.* **1992**, *172*, 305−312.

(17) Chan, M.; Bennick, A. Proteolytic processing of a human salivary proline-rich protein precursor. *Eur. J. Biochem.* **2001**, *268*, 3423−3431.

(18) Hatton, M. N.; Loomis, R. E.; Levine, M. J.; Tabak, L. A. Masticatory lubrification. The role of carbohydrate in the lubricating property of a salivary glycoprotein−albumin complex. *Biochem. J.* **1985**, *230*, 817−820.

(19) Douglas, C. W. I. Bacterial−protein interactions in the oral cavity. *Adv. Dent. Res.* **1994**, *8*, 254−262.

(20) Pascal, C.; Bigey, F.; Ratomahenina, R.; Boze, H.; Moulin, G.; Sarni-Manchado, P. Overexpression and characterization of two human salivary proline rich proteins. *Protein Expression Purif.* **2006**, *47*, 524−532.

(21) Tompa, P. Intrisically unstructured proteins. *Trends Biochem. Sci.* **2002**, *27*, 527−533.

(22) Uversky, V. N. What does it mean to be natively unfolded? *Eur. J. Biochem.* **2002**, *269*, 2−12.

(23) Charlton, A. J.; Baxter, N. J.; Lilley, T. H.; Haslam, E.; McDonald, C. J.; Williamson, M. P. Tannin interactions with a full-length human salivary proline-rich protein display a stronger affinity than with proline-rich repeats. *FEBS Lett.* **1996**, *382*, 289−292.

(24) Murray, N. J.; Williamson, M. P.; Lilley, T. H.; Haslam, E. Study of the interaction between salivary proline-rich proteins and a polyphenol by $^1$H-NMR spectroscopy. *Eur. J. Biochem.* **1994**, *219*, 923−935.

(25) Simon, C.; Barathieu, K.; Laguerre, M.; Schmitter, J. M.; Fouquet, E.; Pianet, I.; Dufourc, E. J. Three-dimensional structure and dynamics of wine tannin−saliva protein complexes. A multitechnique approach. *Biochemistry* **2003**, *42*, 10385−10395.

(26) Jobstl, E.; O'Connell, J.; Fairclough, J. P. A.; Williamson, M. P. Molecular model for astringency produced by polyphenol/protein interactions. *Biomacromolecules* **2004**, *5*, 942−949.

(27) Poncet-Legrand, C.; Edelmann, A.; Putaux, J.-L.; Cartalade, D.; Sarni-Manchado, P.; Vernhet, A. Poly(L-proline) interactions with flavan-3-ols units: Influence of the molecular structure and the polyphenol/protein ratio. *Food Hydrocolloids* **2006**, *20*, 687−697.

(28) Sarni-Manchado, P.; Cheynier, V. Study of noncovalent complexation between catechin derivatives and peptide by electrospray ionization-mass spectrometry (ESI-MS). *J. Mass Spectrom.* **2002**, *37*, 609−616.

(29) Frazier, R. A.; Papadopoulou, A.; Mueller-Harvey, I.; Kissoon, D.; Green, R. J. Probing protein−tannin interactions by isothermal titration microcalorimetry. *J. Agric. Food Chem.* **2003**, *51*, 5189−5195.
(30) Frazier, R. A.; Papadopoulou, A.; Green, R. J. Isothermal titration calorimetry study of epicatechin binding to serum albumin. *J. Pharm. Biomed. Anal.* **2006**, *41*, 1602−1605.
(31) Charlton, A.; Baxter, N. J.; Khan, M. L.; Moir, A. J. G.; Haslam, E.; Davis, A. P.; Williamson, M. P. Polyphenol/peptide binding and precipitation. *J. Agric. Food Chem.* **2002**, *50*, 1593−1601.
(32) Flanzy, C. *Oenologie*—Fondements scientifiques et technologiques, Technique et Documentation ed.; Lavoisier: Paris, 1998; p 1311.
(33) Gal, J. Y.; Fovet, Y.; Adib-Yadzi, M. About a synthetic saliva for in vitro studies. *Talanta* **2001**, *53*, 1103−1115.
(34) Sapan, C. V.; Lundblad, R. L.; Price, N. C. Colorimetric protein assay techniques. *Biotechnol. Appl. Biochem.* **1999**, *29*, 99−108.
(35) Gun'ko, V. M.; Klyueva, A. V.; Levchuk, Y. N.; Leboda, R. Photon correlation spectroscopy investigations of proteins. *Adv. Colloid Interface Sci.* **2003**, *105*, 201−328.
(36) Baxter, N. J.; Williamson, M. P.; Lilley, T. H.; Haslam, E. Stacking interactions between caffeine and methyl gallate. *J. Chem. Soc., Faraday Trans.* **1996**, *92*, 231−234.
(37) Wroblewski, K.; Muhandiram, R.; Chakrabartty, A.; Bennick, A. The molecular interaction of human salivary histatins with polyphenolic compounds. *Eur. J. Biochem.* **2001**, *268*, 4384−4397.
(38) Kentsis, A.; Mezei, M.; Osman, R. Origin of the sequence-dependent polyproline II structure in unfolded peptides. *Proteins: Struct., Funct., Bioinf.* **2005**, *61*, 769−776.
(39) Receveur-Brechot, V.; Bourhis, J. M.; Uversky, V. N.; Canard, B.; Longhi, S. Assessing protein disorder and induced folding. *Proteins: Struct., Funct., Bioinf.* **2006**, *62*, 24−45.
(40) Fuxreiter, M.; Simon, I.; Friedrich, P.; Tompa, P. Preformed structural elements feature in partner recognition by intrinsically unstructured proteins. *J. Mol. Biol.* **2004**, *338*, 1015−1026.
(41) Dyson, H. J.; Wright, P. E. Coupling of folding and binding for unstructured proteins. *Curr. Opin. Struct. Biol.* **2002**, *12*, 54−60.
(42) Fink, A. L. Natively unfolded proteins. *Curr. Opin. Struct. Biol.* **2005**, *15*, 35−41.
(43) van Rensburg, H.; Steynberg, P. J.; Burger, J. F. W.; van Heerden, P.; Ferreira, D. Circular dichroic properties of flavan-3-ols. *J. Chem. Res.* **1999**, *7*, 450−451.
(44) Tompa, P. Intrinsically unstructured proteins evolve by repeat expansion. *Bioessays* **2003**, *25*, 847−855.
(45) Haslam, E. Natural polyphenols (vegetable tannins) as drugs: possible modes of action. *J. Nat. Prod.* **1996**, *59*, 205−215.

**Received for review February 12, 2007. Revised manuscript received April 6, 2007. Accepted April 8, 2007.**

JF0704108